AIAA 81-0682R

Current Distribution on the Electrodes of MPD Arcjets

Itsuro Kimura,* Kyoichiro Toki,† and Masafumi Tanaka‡
University of Tokyo, Tokyo, Japan

Current distribution on the electrodes of a conventional MPD arcjet without external magnetic field was calculated based on induction equation, with the assumption that the magnetic Reynolds number is small. The calculated result, which showed the influence of tensor conductivity, coincided fairly well with the corresponding experimental one. It was seen, however, that the current density near the cathode tip in experiment had a larger value than that in calculation. This discrepancy was explained tentatively as being the result of the occurrence of cathode spots. It is also suggested in this paper that the unfavorable current concentration at the cathode base can be suppressed by using a specially devised divided cathode.

Introduction

THE current distribution and electromagnetic acceleration in MPD arcjets have received considerable attention recently, and a number of theoretical and experimental investigations have been conducted.[1-5] This theoretical and experimental study places emphasis on the phenomena involved near the electrodes in a conventional MPD arcjet with a solid cathode. The information on the current distribution in the region near the cathode of an MPD arcjet is of vital importance in understanding the thrust-producing mechanism and in evaluating the effect of erosion in long-time operation or a large number of pulsed operations.

Theoretical Analysis

Assumptions and Basic Equations

The theoretical analysis was conducted for the electrode geometry used in the experiments (Fig. 1), the results of which will be described later. Under the following assumptions, the current distributions and, hence, the current densities on the electrode surfaces were investigated:

1) The current flow is stationary and axisymmetric; this assumption means that in the present analysis unsteady phenomena such as current spots are not taken into consideration.

2) The plasma properties are uniform in the discharge region.

3) No external magnetic field is applied, and magnetic field originates only from the discharge current.

4) The effect of the electrical sheath formed at the surface of electrodes is neglected.

5) The effect of flow of plasma can be neglected.

The general induction equation, which is derived by taking the curl of Ohm's law, is written in the form[6]

$$\frac{\partial \boldsymbol{B}}{\partial t} + \nabla \times \frac{\nabla \times \boldsymbol{B}}{\mu_0 \sigma} - \nabla \times (\boldsymbol{v} \times \boldsymbol{B}) + \nabla \times \left[\frac{\beta}{\mu_0} (\nabla \times \boldsymbol{B}) \times \boldsymbol{B} \right] = 0 \tag{1}$$

The nondimensional form of this equation is expressed as

$$\frac{\partial \tilde{\boldsymbol{B}}}{\partial \tilde{t}} = \tilde{\nabla} \times (\tilde{v} \times \tilde{\boldsymbol{B}}) - \frac{1}{Rm} \left[\tilde{\nabla} \times \frac{\tilde{\nabla} \times \tilde{\boldsymbol{B}}}{\tilde{\sigma}} + \omega\tau\tilde{\beta} \tilde{\nabla} \times \{ (\tilde{\nabla} \times \tilde{\boldsymbol{B}}) \times \tilde{\boldsymbol{B}} \} \right] \tag{2}$$

where

$$\tilde{x} = \frac{x}{L_0}, \quad \tilde{t} = \frac{t}{L_0/v_0}, \quad \tilde{\boldsymbol{B}} = \frac{\boldsymbol{B}}{B_0}, \quad \tilde{\sigma} = \frac{\sigma}{\sigma_0}, \quad \tilde{\beta} = \frac{\beta}{\beta_0}, \quad \tilde{v} = \frac{v}{v_0}$$

and $Rm = \mu_0 \sigma_0 v_0 L_0$ is the magnetic Reynolds number and $\omega\tau$ the Hall parameter.

In the situation of the experiments described in this paper, the value of Rm is in the range of $0.01 \sim 0.1$ in the discharge region near the cathode. Thus, under the assumption of steady state, the induction equation can be simplified as

$$\nabla \times (\nabla \times \boldsymbol{B}) + \sigma\beta \nabla \times \{ (\nabla \times \boldsymbol{B}) \times \boldsymbol{B} \} = 0 \tag{3}$$

The parameter $\sigma\beta$ ($\sigma = e^2 n_e / m_e \nu$, $\beta = 1/en_e$), which is equal to $e/m_e\nu$, can be expressed as $\omega\tau/B$, where B is self-induced magnetic field strength. The azimuthal component of Eq. (3) is expressed

$$\frac{\partial^2 B_\theta}{\partial r^2} + \frac{\partial^2 B_\theta}{\partial z^2} + \frac{1}{r}\frac{\partial B_\theta}{\partial r} + \frac{\sigma\beta}{r}\frac{\partial (B_\theta^2)}{\partial z} - \frac{B_\theta}{r^2} = 0 \tag{4}$$

where B_θ is the azimuthal component of $\boldsymbol{B}$ ($B_r = B_z = 0$ from assumption 1) or

$$\frac{\partial^2 \psi}{\partial r^2} + \frac{\partial^2 \psi}{\partial z^2} - \frac{1}{r}\frac{\partial \psi}{\partial r} + \frac{2\sigma\beta\psi}{r^2}\frac{\partial \psi}{\partial z} = 0 \tag{5}$$

with $rB_\theta = \psi$.

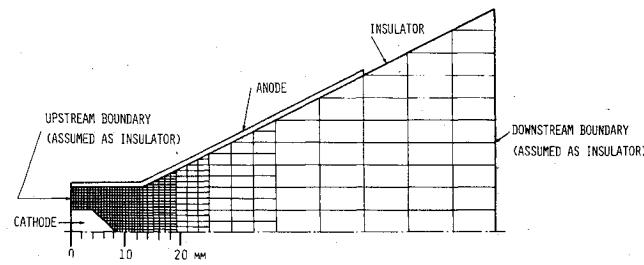

Fig. 1 Electrodes configuration and mesh for numerical calculation (cathode-tip angle, 90 deg; anode-nozzle divergence angle, $2\tan^{-1}(1/2) \simeq 53$ deg).

Presented as Paper 81-0682 at the AIAA/JSASS/DGLR 15th International Electric Propulsion Conference, Las Vegas, Nev., April 21-23, 1981; submitted April 29, 1981; revision received Nov. 12, 1981.

*Professor, Dept. of Aeronautics, Faculty of Engineering. Member AIAA.

†Graduate Student, Dept. of Aeronautics (presently Research Scientist, National Aerospace Laboratory, Kakuda, Japan).

‡Graduate Student, Dept. of Aeronautics, Faculty of Engineering.

Using Maxwell's $\nabla \times B$ relation, the radial and axial components of current density are expressed in terms of ψ,

$$j_r = -\frac{1}{\mu_0}\frac{\partial B_\theta}{\partial z} = -\frac{1}{\mu_0 r}\frac{\partial \psi}{\partial z} \tag{6}$$

$$j_z = \frac{1}{\mu_0 r}\frac{\partial (rB_\theta)}{\partial r} = \frac{1}{\mu_0 r}\frac{\partial \psi}{\partial r} \tag{7}$$

These equations show that ψ is a stream function in a cylindrical coordinate system. Using these equations and Ohm's law, the components of electric field are also expressed in terms of ψ

$$E_r = -\frac{1}{\sigma\mu_0 r}\frac{\partial \psi}{\partial z} - \frac{\beta\psi}{\mu_0 r^2}\frac{\partial \psi}{\partial r} \tag{8}$$

$$E_z = \frac{1}{\sigma\mu_0 r}\frac{\partial \psi}{\partial r} - \frac{\beta\psi}{\mu_0 r^2}\frac{\partial \psi}{\partial z} \tag{9}$$

The boundary conditions are as follows. On the electrode surfaces, E is perpendicular to the surfaces. On the insulator surfaces, ψ is constant, because $j_\perp$ is equal to zero. At the upstream boundary (assumed as insulator), $\psi = -\mu_0 J/2\pi \equiv \psi_0$ (J is the total discharge current) from Maxwell's $\nabla \times B$ relation. At the downstream boundary (assumed as insulator) and at the surface of insulator which constitutes the downstream part of anode nozzle, ψ is assumed to be zero. Furthermore, on the center line ($r=0$), ψ is equal to zero.

It must be noticed here that in the nondimensional expression of Eq. (5) and the boundary conditions, $\sigma\beta\psi_0/L_0$ appears as only one similarity parameter.

Calculated Results

The solutions of Eq. (5) under these boundary conditions can be obtained by the finite-differential method, using successive approximation method for the evaluation of the nonlinear term. Figures 2 and 3 show the current density on the cathode and anode surfaces, respectively, in the cases of discharge currents of 500, 1000, and 2000 A for $\sigma\beta = 0$, 50, 100 T^{-1}, taking the distance from the upstream boundary abscissa. It is seen that, with the increase of $\sigma\beta$ ($=\omega\tau/B$), at the upstream part of the cathode surface the current density increases and, at that of the anode surface, vice versa. It must be noticed here that the degree of current concentration at the cathode tip is insensitive to the increase of $\sigma\beta$.

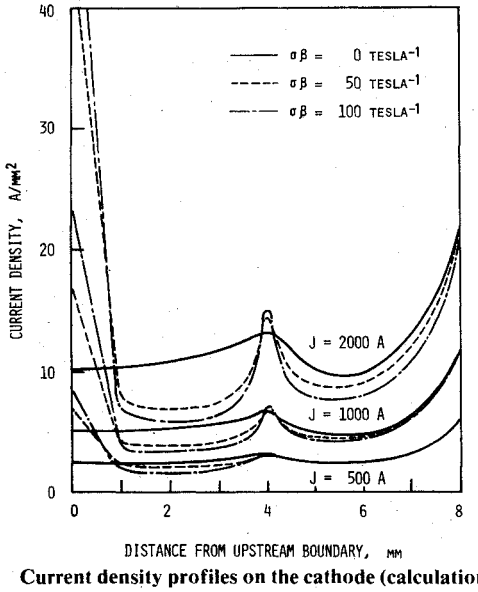

Fig. 2 Current density profiles on the cathode (calculation).

Experimental Investigation

Apparatus and Experimental Procedure

Figure 4 is a schematic of the MPD arcjet used for the experimental investigation. The configuration of the electrodes has the same geometry with that in the theoretical analysis. The nozzle-shaped copper anode has a throat diameter of 16 mm and the tungsten solid-cathode with a conical tip has an outer diameter of 8 mm. The arcjet was operated in quasisteady mode (operation time: 3 ms). Argon propellant was injected through the annular slit at the interelectrodes insulator and the background pressure was maintained at about 5×10^{-2} Torr.

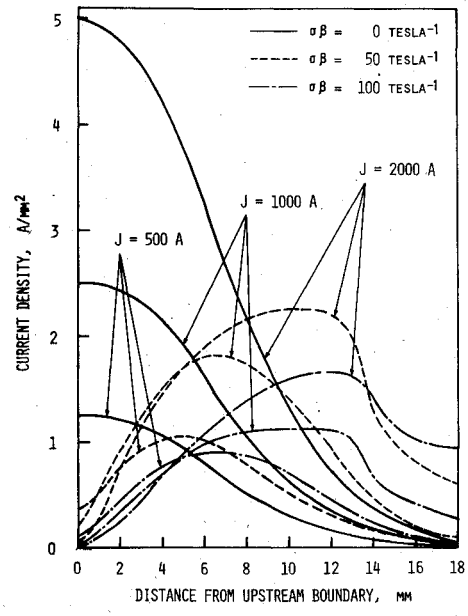

Fig. 3 Current density profiles on the anode (calculation).

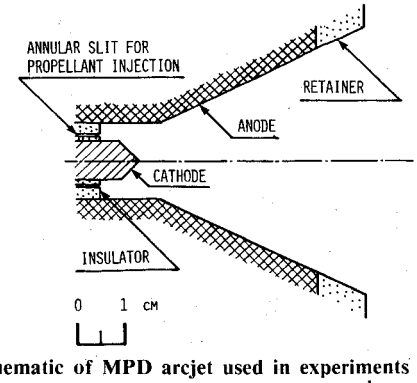

Fig. 4 Schematic of MPD arcjet used in experiments (cathode-tip angle, 90 deg; anode-nozzle divergence angle, $2\tan^{-1}(1/2) \simeq 53$ deg).

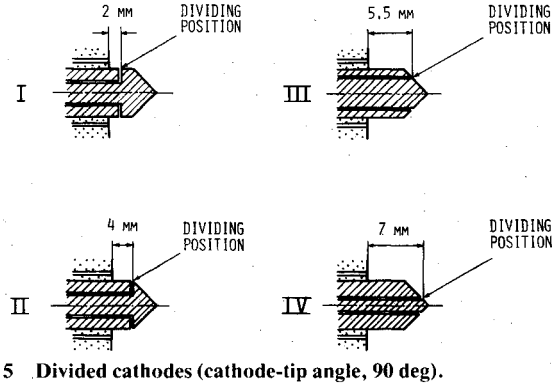

Fig. 5 Divided cathodes (cathode-tip angle, 90 deg).

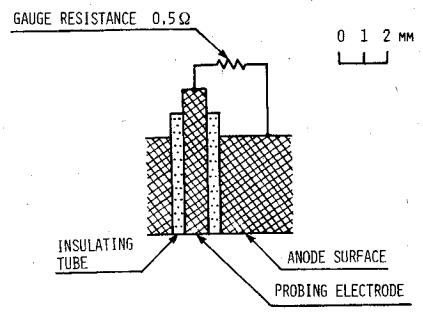

Fig. 6 Probing electrode at the anode.

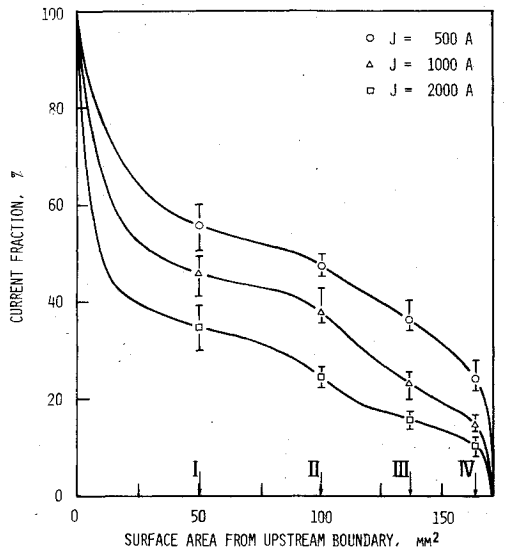

Fig. 7 Current fraction into the inner part of the divided cathode (experiment).

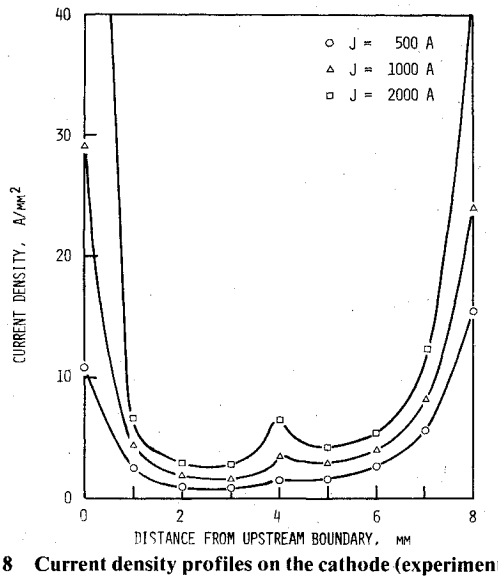

Fig. 8 Current density profiles on the cathode (experiment).

The current distributions on the cathode surface were measured by using four types (I-IV) of divided cathodes (tungsten) as shown in Fig. 5. In the measurements, it was confirmed that the connecting resistances of the outer and inner parts of a divided cathode to the power line were less than 1 mΩ, and the currents flowing through each part were measured by Rogowsky coils. The current distributions on the anode surface were measured by furnishing electrically insulated small electrodes flush with the anode surface as shown

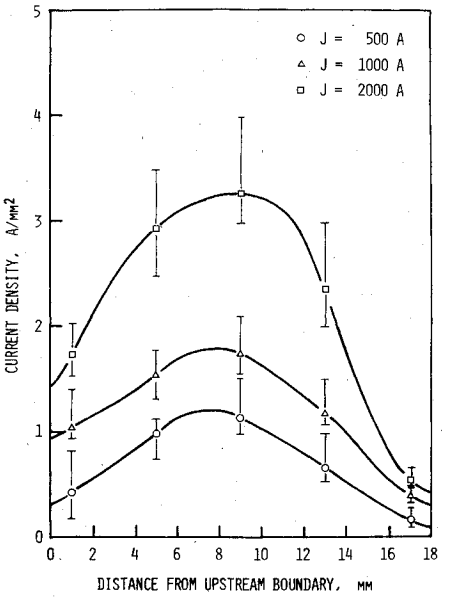

Fig. 9 Current density profiles on the anode (experiment).

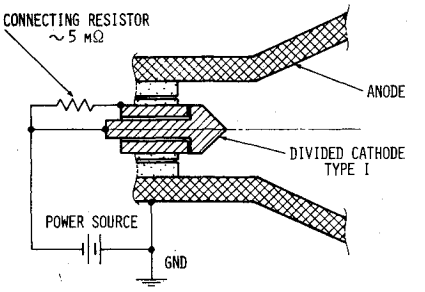

Fig. 10 Method proposed to decrease the current concentration at the cathode base.

in Fig. 6. The voltage change caused by 0.5 Ω gage resistance was always less than 1 V. Details of these methods are described elsewhere.[4,5]

Experimental Results

Figure 7 shows the experimental results obtained using divided cathodes for discharge currents of 500, 1000, and 2000 A at a mass flow of 30 mg/s. The ordinate shows the current fraction which flows into the inner part of divided cathode and the Roman numerals in the abscissa represent the dividing positions at the cathode surface. It was generally observed that, although the oscillograms of total discharge currents did not show any fluctuation, the oscillograms of the currents to the inner part and hence the outer part of the divided cathodes showed fluctuations of several kilocycles, as in the cases of hollow-cathode experiments.[5] This fluctuation may suggest an instability of current attachment to cathode surface, such as nonstationary spot phenomena. In Fig. 7, the scale of abscissa is taken to be proportional to the cathode surface area measured from the cathode base (the edge of the interelectrodes insulator). In Fig. 8, the distribution of current density on the cathode surface deduced from Fig. 7 is shown. In this figure, the scale of abscissa indicates the axial distance from the cathode base. It is seen in this figure that the high current density occurs at the cathode base as well as at the cathode tip.

Figure 9 shows the current density distribution on the anode surface, taking the axial distance from the upstream boundary (the edge of the interelectrodes insulator) abscissa. In this figure, it is seen that the maximum of current density appears at the inside part of the anode throat.

Discussion

Comparing the theoretical results with the experimental ones, it is seen that the theoretical results under the large value of $\sigma\beta$ can approximate the actual current distributions on the electrode surfaces fairly well at the different discharge currents. And as for the value of $\sigma\beta$ under the situation of the present experiment, it was also confirmed, using the data based on Langmuir probe measurement, that it is on the order of 10^2. Thus, it may be concluded that the parameter $\sigma\beta$ has the most importance for the current distributions on the electrode surfaces, within the range of present investigation. It must be also noticed, however, that the actual current density at the cathode tip is somewhat higher than the theoretical prediction. One of the causes of this discrepancy may be the current spot phenomenon; intense spots can easily drift toward the cathode tip because of Lorentz force and distort the current distribution on the cathode surface.[7] We also suppose that the nonuniformity of plasma conductivity and temperature profile over the cathode surface, or inequality in sheath formation, may affect the current distribution on the cathode.

In the practical point of view, it is preferable to suppress the current concentration at the cathode base because it degrades the efficiency and the lifetime of the MPD arcjet. As one of the solutions for this point, it must be noticed that, when the divided cathode of type I has an increased connecting resistor of outer part (order of 5 mΩ), it is possible to decrease the current to the outer part,[8] which involves the cathode base, without noticeable increase of loss of electrical power (Fig. 10). Detailed results about this matter will be reported later.

Conclusions

Current distributions on the electrodes of an MPD arcjet without external magnetic field were calculated numerically, with the assumption that the magnetic Reynolds number is small. It was found that, with the increase of $\sigma\beta$ $(=\omega\tau/B)$, at the upstream part of cathode surface the current density increases and at that of anode surface, vice versa. In the range of $\sigma\beta = 10^2\ T^{-1}$, numerical results give a good approximation to the actual current distributions on the electrodes, except that actual current density near the cathode tip had a larger value than that of numerical result. This matter may be explained as the result of the current spot phenomenon observed on the cathode surface. From the practical point of view, it was also suggested that the current concentration on the cathode base can be decreased by using an appropriate type of divided cathode with an increased connecting resistor for its outer part.

Acknowledgment

The authors give thanks to Dr. Yoshihiro Arakawa, Akira Tanaka, and Yasushi Chikatani for useful discussions in the course of this investigation.

References

[1] Krülle, G., "Theoretical Treatment of Current, Mass Flow, and Related Distributions in MPD Plumes," AIAA Paper 72-501, 1972.

[2] Hügel, H., Maisenhälder, F., and Schock, W., "Investigations of Plasma Flows Accelerated by the Self-Magnetic Effect," AIAA Paper 70-1098, 1970.

[3] Jahn, R. G., Clark, K. E., Oberth, R. C., and Turchi, P. J., "Acceleration Patterns in Quasi-Steady MPD Arcs," *AIAA Journal*, Vol. 9, Jan. 1971, pp. 167-172.

[4] Kimura, I. and Arakawa, Y., "Effect of Applied Magnetic Field on Physical Processes in an MPD Arcjet," *AIAA Journal*, Vol. 15, May 1977, pp. 721-724.

[5] Toki, K. and Kimura, I., "Studies of Current Distribution on the Hollow Cathode of an MPD Arcjet," AIAA Paper 79-2113, 1979.

[6] Sutton, G. W. and Sherman, A., *Engineering Magnetohydrodynamics*," McGraw-Hill Book Co., New York, 1965, pp. 302-308.

[7] Hügel, H., "Experimental Investigations on Cathodes of Plasma Thrusters with Self-Magnetic Acceleration," *Proceedings of the VIIth International Conference on Phenomena in Ionized Gases*, Vol. 3, Gradevinska Knjiga Publishing House, Beograd, 1966, pp. 350-354.

[8] Toki, K., "Current Distribution on the Hollow Cathode of an MPD Arcjet," Doctorial Thesis, University of Tokyo, Japan, 1981.